Influence of Montmorillonite Treatment and Montmorillonite Dispersion State on the Crystallization Behavior of Poly(ethylene terephthalate)/Montmorillonite Nanocomposites

Ming Yin,[1,2] Chuncheng Li,[1] Guohu Guan,[1] Dong Zhang,[1] Yaonan Xiao[1]

[1]*Beijing National Laboratory for Molecular Sciences, CAS Key Laboratory of Engineering Plastics, Institute of Chemistry, the Chinese Academy of Sciences, Beijing 100190, People's Republic of China*
[2]*Graduate University of the Chinese Academy of Sciences, Beijing 100049, People's Republic of China*

Received 8 October 2008; accepted 4 May 2009
DOI 10.1002/app.30714
Published online 2 July 2009 in Wiley InterScience (www.interscience.wiley.com).

ABSTRACT: TiO_2/SiO_2 sol was intercalated into montmorillonite (MMT), which was pretreated with polyvinylpyrrolidone (PVP). A series of poly(ethylene terephthalate) (PET)/MMT hybrids were prepared using the obtained MMT as polycondensation catalysts. X-ray diffraction (XRD) results proved that MMT dispersion states could be controlled by the amount of TiO_2/SiO_2 sol that was incorporated into MMT, ranging from agglomeration to exfoliation. The crystallization behavior of PET/MMT composites synthesized in this study was characterized by differential scanning calorimeter (DSC), polarized optical microscope (POM) and scanning electron microscopy (SEM) to clarify the effects of clay treatment and its dispersion state on the crystallization behavior of the PET substrate. The results indicated that MMT treated with less PVP would retain relatively higher nucleation efficiency while when MMT containing more PVP, the nucleation effect of MMT became weaker. If MMT formed big grains within PET substrate, the disturbance of the growing crystals was negligible; but the exfoliation of MMT layers would greatly magnify the spatial constraint which would slow down the crystallization process of PET matrix. For certain exfoliated PET/MMT composites, the crystallization rate was even lower than that of pure PET though clay content was low. © 2009 Wiley Periodicals, Inc. J Appl Polym Sci 114: 2327–2338, 2009

Key words: Poly(ethylene terephthalate); nanocomposites; crystallization; clay

INTRODUCTION

Poly(ethylene terephthalate) (PET) is one of the most extensively used semicrystal polymers, which has found its applications in fibers, films, packaging and molding materials.[1–4] The crystallization behavior of PET greatly affects the process parameters and the properties of the obtained materials. Recently, many research groups have devoted their efforts to the study of PET/montmorillonite (MMT) nanocomposites. The incorporation of MMT not only improves the properties of PET,[5–10] but also greatly alters the crystallization behavior of the PET substrate.[3,4,11–15] So it is of great importance to research the crystallization processes of PET/MMT composites.

Most reports considered the MMT layers within PET/MMT hybrids as an effective nucleating agent, the crystallization rate of the composites was remarkably improved due to the heterogeneous nucleation of the clay particles. Qi and coworkers[3] had reported the preparation of PET/MMT nanocomposite which had three times greater crystallization rate than that of pure PET. Though the clay sheets acted as impediment of the growing crystals simultaneously, the nucleation effect of MMT could overrun the hindrance effect. As a result, clay could accelerate the overall crystallization of PET and the composites could be used for applications involving high-speed processing such as injection molding.

However, too fast crystallization rate and higher crystallinity may cause some undesired properties of the final products in some cases. For example, PET/clay nanocomposites have been considered for the application in food/beverage packaging and medical field recently due to the dramatically decreased oxygen and carbon dioxide permeability by the addition of clay.[6,7] However, these nano-scale fillers greatly enhance the crystallization rate of PET matrix and increase the crystallinity of the material, resulting in increase of haze of the final products, especially at high clay loading levels, which greatly limit the application of PET/MMT nanocomposites as food/beverage packaging.[16,17] So it is of great importance to control the crystallization rate of PET/MMT

Correspondence to: C. Li (lichch@iccas.ac.cn).

nanocomposites for different use by variation of the clay treatment while the clay dispersion state remains exfoliation.

In this study, the key objective is to investigate the effects of clay treatment and clay dispersion state on the crystallization behavior of PET/MMT composites. A series of MMT treated with different amount of PVP and TiO_2/SiO_2 sol were prepared, PET/MMT composites were synthesized using these treated MMT as polycondensation catalysts. X-ray diffraction (XRD) curves confirmed that MMT treatment determined its dispersion state. Clay treatment and clay dispersion state, two main factors that influenced crystallization behavior of PET/MMT composites, were studied respectively. The effect of clay treatment on the crystallization behavior of PET matrix was studied while the clay dispersion state was the same; the crystallization process of the hybrids possessing different clay dispersion states was researched while the corresponding clay based catalysts were treated with constant quantity of PVP. The results indicated that the crystallization rates of the exfoliated nanocomposites with the same clay contents varied a lot according to the clay treatment. For certain exfoliated sample, the crystallization rate was even lower than that of pure PET. Though some researchers have reported that increasing clay loading in an exfoliated PET/MMT composite would lead to decreased crystallization rate (still higher than the crystallization rate of pure PET), this phenomenon usually became prominent at high clay content for PET/MMT composites, often larger than 10%[4], far beyond the range of this study. Also the crystallization behavior of completely exfoliated PET/MMT nanocomposites has seldom been reported, especially the nanocomposites were prepared using *in situ* methods and clay supported catalysts, so this work could be a complement of the published results.

EXPERIMENTAL

Materials

Sodium-montmorillonite (Na-MMT) with a cation exchange capacity of 100 meq/100 g and a nominal particle size of 40 μm was purchased from Zhangjiakou Clay Mineral Corp. (Hebei Province, People's Republic of China). Dimethyl terephthalate (DMT) was a commercial product from Mitsubishi Chemical Corp. (Tokyo, Japan). Polyvinylpyrrolidone (PVP) (AR, 98%, impurity is mainly water), tetrabutyl titanate ($Ti(OC_4H_9)_4$) (AR, 99%), tetraethoxide orthosilicate (TEOS) (AR, 98%) and ethylene glycol (EG) (AR, 99%) were purchased from Beijing Chemical Reagents Company (China). The chemicals were used as received.

Preparation of the catalyst

A series of MMT based catalysts were synthesized. Since the preparation procedures were similar, only one typical synthesis process is given here as an example. First, 1 g of PVP, 400 g of deionized water and 4 g of Na^+– montmorillonite (Na-MMT) were placed into a 500 mL three-neck flask. The mixture was vigorously stirred for 6 h and the temperature was maintained at 85°C. The precipitate was isolated by centrifugation and washed with 200 mL distilled water three times. Then the acquired organo-clay was dried in vacuum to a constant weight at 80°C and grounded into powder, screened with a 300-mesh sieve.

Second, the obtained PVP-MMT would be intercalated by TiO_2/SiO_2 sol. The sol-intercalated clay was prepared as the following procedures reported by Yamanaka et al.[18,19] The silicon hydrate sol solution was prepared by mixing $Si(OC_2H_5)_4$ (TEOS), 2 mol/L HCl and ethanol in a ratio of 10.4 g : 2.5 mL : 3 mL at room temperature. Titanium hydrate sol was obtained through the hydrolysis of tetrabutyl titanate ($Ti(OC_4H_9)_4$) in 1 mol/L HCl solution and the molar ratio of HCl to $Ti(OC_4H_9)_4$ was about 4. The resulting slurry was peptized to a clear sol solution by continuous stirring for 3 h at room temperature. The two sol solutions were then mixed and stirred for 30 min at room temperature. Subsequently, the mixture was added into the 1 wt % suspension of the pretreated clay, in a ratio of 0.1 mmol : 1 g for Ti/clay. The slurry was stirred for 6 h to maximize the intercalation, and then the solid was separated by centrifugation and washed with deionized water until no Cl^- could be detected out of the liquid phase by one drop of $AgNO_3$ solution. The wet cake was dried under vacuum to a constant weight at 80°C and grounded into powder, screened with a 300-mesh sieve. The powder was named P0.25-Ti0.1-MMT. The composition and synthesis parameters of the other samples are listed in Table I.

Synthesis of PET/ MMT nanocomposite

Only one typical example is given here. 101 g of DMT and 72 g of EG) were added into a home made four-neck flask equipped with a mechanical

TABLE I
The Treatment Parameters of the Catalysts

Samples	PVP/MMT (wt/wt)	Ti (mmol)/ Clay (g)
P0.25-Ti0.1-MMT	0.25	0.1
P0.25-Ti0.2-MMT	0.25	0.2
P0.25-Ti0.3-MMT	0.25	0.3
P0.5-Ti0.3-MMT	0.5	0.3
P1.0-Ti0.2-MMT	1.0	0.2

TABLE II
Composition of the Composites

Samples	Clay type	Clay loading (wt %)	Intrinsic viscosity (η) (dl/g)
Pure PET	/	/	0.63
PET/Na-MMT	Na-MMT	2	0.68
P0.25-Ti0.1	P0.25-Ti0.1-MMT	2	0.67
P0.25-Ti0.2	P0.25-Ti0.2-MMT	2	0.65
P0.25-Ti0.3	P0.25-Ti0.3-MMT	2	0.71
P0.5-Ti0.3	P0.5-Ti0.3-MMT	2	0.73
P1.0-Ti0.2	P1.0-Ti0.2-MMT	2	0.69
2P0.25-Ti0.3	P0.25-Ti0.3-MMT	4	0.68

stir, 0.03 g of manganese acetate was added as catalyst. The four-neck flask was made of glass and heated by alloy metal bath, the heater is monitored by a temperature-control device. The mixture was heated to about 180°C under the protection of continuous flow of nitrogen whereupon methanol was generated. After a theoretical amount of methanol was removed, the transesterfication step was finished. Then 2 g of P0.25-Ti0.1-MMT was added and the temperature of the reaction system was increased to 280°C. At the same time, a vacuum was applied (<50 Pa). The polycondensation step was finished until the mechanical stir reached a certain torque. All the polymerizations could be done within 2 h. Pure PET was also synthesized in our lab with the same method but no organo-MMT powder was added, instead, 0.03 g of antimony trioxide was added as polycondensation catalyst. PET/Na-MMT was prepared by adding 2 g of Na-MMT and 0.03 g of antimony trioxide into the reaction system after the transesterfication step was finished. The specifications of the samples are listed in Table II.

Characterization

XRD was performed at room temperature by a Rigaku Model D/max-2B diffractometer using Cu Kα radiation ($\lambda = 0.154$ nm) at a generator voltage of 20 kV and a generator current of 200 mA. Testing data were collected from 1.5 to 40° at a scanning rate of 2°/min.

Thermogravimetric analysis (TGA) was performed on a Perkin–Elmer TGA7. Samples were heated at a rate of 20°C/min from 50 to 700°C in a nitrogen atmosphere. The standard uncertainty of decomposition temperature is ±1°C.

The intrinsic viscosity (η) of all the samples was measured at 25°C ± 0.1°C in a Ubbelohde viscometer, with the mixture of 50/50 (wt/wt) phenol/1,1,2,2- tetrachloroethane as solvent.

Chemical composition of the pristine clay and the clay based catalysts was determined using an electron probe microanalyzer (EPMA) JXA-8800R (JEOL). Before EPMA measurements, all the samples were dried at 80°C under vacuum to remove absorbed water, and then the clays were molded into a shape of disk. Acceleration voltage was 20 kV, beam current was 20 nA and beam diameter was 5 μm. The peak counting time was 10 s and 10 s for the background.

A Perkin–Elmer DSC-7 differential scanning calorimeter (DSC) thermal analyzer was used for DSC analysis. Each sample, about 3 mg, was accurately weighted before being placed in DSC span. All DSC measurements were performed under dry nitrogen atmosphere. For isothermal process, samples were first heated from room temperature to 290°C with a heating rate of 40°C/min and kept at 290°C for 5 min to eliminate any thermal history, then rapidly cooled to designated crystallization temperatures, and held at this temperature until crystallization was completed. Isothermal crystallization of PET/MMT nanocomposites and pure PET were performed under various temperatures ranging from 208°C to 216°C. For the programmed cooling process, all samples were first held at 290°C for 5 min, and then cooled at 10°C/min to 50°C.

The crystallization process of pure PET and PET/MMT composites was studied using an Olympus BX51 polarized optical microscope (POM) connected with a Linkam THMS600 hot stage under nitrogen atmosphere. The cooling rate was controlled with the aid of liquid nitrogen. The sample films were first melted at 290°C and held at that temperature for 5 min to eliminate residual crystals, then cooled to 35°C at 10°C/min. The polarized optical micrographs were taken every two seconds once the cooling process started. The samples used for POM observation were films with thickness of about 30 μm, which were prepared with a home made compression molder under vacuum at 280°C.

The crystalline morphology of pure PET and PET/MMT nanocomposite (P0.25-Ti0.3) was examined with a Leica MPS 30 polarizing optical microscope and a Hitachi S-530 scanning electron microscope. The sample films were first melted at 290°C and held at that temperature for 5 min to eliminate residual crystals, cooled to 230°C at 100°C/min and held at 230°C for 60 min, and then quenched to 35°C for observation. All the thermal treatment was done on Linkam THMS600 hot stage under dry nitrogen atmosphere. The thin sample pieces for scanning electron microscopy (SEM) examination were prepared using the same method except that they were much thicker than those for POM observation. These thick pieces were chemically etched with a solution of 5/95 (wt/wt) potassium hydroxide/methanol. They were coated with platinum before SEM observation.

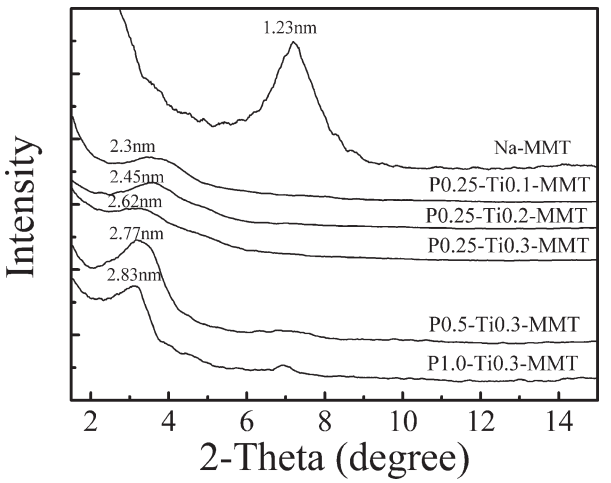

Figure 1 XRD curves of the raw MMT and the MMT based polycondesation catalysts.

RESULTS AND DISCUSSION

Characterization of the catalysts and composites

Figure 1 represented the XRD curves of raw MMT and the MMT based polycondensation catalysts. It can be seen that the d(001) peak of the raw clay appeared at $2\theta \approx 7.2^\circ$, corresponding to the basal spacing of 1.23 nm. After the treatment of PVP and TiO_2/SiO_2 sol, the *d*(001) peaks of MMT at 7.2° shifted toward lower angles, shown at about 3°, corresponding to the basal spacing of approximate 2.6 nm. The increase of the interlayer spacings obviously meant that PVP was suitable in the organification of raw MMT. The amount of PVP introduced into MMT could be controlled according to the results of TGA study, which was summarized in Table III. Apparently, MMT based polycondensation catalysts pretreated with higher amount of PVP had less weight residual at 700°C, which meant that these samples had relatively higher organic content. The initial decomposition temperatures of the catalysts were far beyond the polycondensation temperature of PET, so the catalysts would not decompose during the *in situ* synthesis of PET/MMT composites. Also, according to Table IV, the TiO_2/SiO_2 sol was successfully intercalated into the clay galleries

TABLE III
TGA Results of the Catalysts

Samples	Weight residual at 700°C	Initial decomposition temperature (°C)
Na-MMT	96.1%	/
P0.25-Ti0.1-MMT	82.9%	403
P0.25-Ti0.2-MMT	82.4%	402
P0.25-Ti0.3-MMT	82.3%	403
P0.5-Ti0.3-MMT	76.4%	401
P1.0-Ti0.2-MMT	72.0%	398

TABLE IV
EPMA Results of Raw MMT and the Catalysts

Samples	Na_2O (wt %)	TiO_2 (wt %)
Na-MMT	2.89	0.08
P0.25-Ti0.1-MMT	0.20	0.55
P0.25-Ti0.2-MMT	0.18	1.16
P0.25-Ti0.3-MMT	0.14	1.52
P0.5-Ti0.3-MMT	0.23	1.58
P1.0-Ti0.2-MMT	0.22	1.35

as indicated by EPMA tests. After the treatment with TiO_2/SiO_2 sol, the content of the exchangeable cations of PVP treated MMT, such as Na^+, which located between the neighboring clay lamellas, drastically reduced. Its content decreased to about one tenth of the original value. Meanwhile, the titanium content increased dramatically. Since PVP was a nonionic polymer and physically absorbed onto MMT,[20,21] Na^+ should be exchanged by the positively charged TiO_2/SiO_2 sol particles.[18,22] Besides, in this study, SiO_2 sol particles acted as the carrier of TiO_2 to increase the size of TiO_2 particles, so the TiO_2 sol could cover a much larger area of MMT layers and disperse homogeneously throughout the clay,[18,19,22] which could facilitate the exfoliation of MMT.

After polymerization, the d (001) peaks of the clay based catalysts moved to lower angles and their intensity dramatically decreased, as shown by Figure 2, which indicated that polymer chains had penetrated into the clay interlayer spaces, the distance between neighboring MMT platelets was enlarged and the clay stacks lost some of their periodic structures. For 2P0.25-Ti0.3, P0.25-Ti0.3, P0.5-Ti0.3, and P1.0-Ti0.2, the 2θ diffraction peaks were completely lost, suggesting that satisfactory degree of exfoliation was achieved, clay monolayers dispersed homogeneously throughout the polymer matrix. For P0.25-Ti0.2, a wide hump could be observed between 2

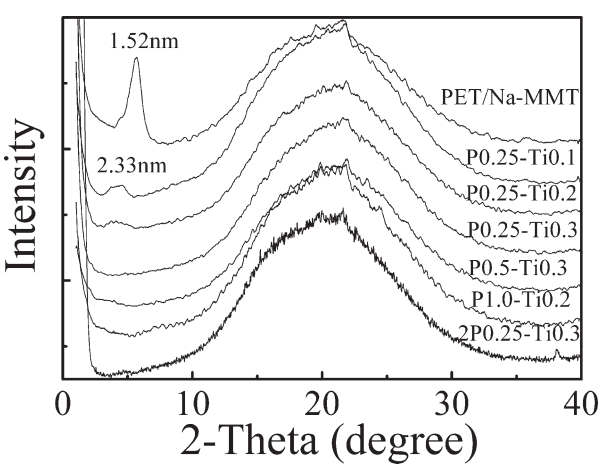

Figure 2 XRD curves of PET/MMT composites.

and 5°, indicating intercalated structure. As for P0.25-Ti0.1, a weak diffraction of MMT was seen, which meant that MMT formed agglomerated structure. Untreated MMT must have formed big grains in PET/Na-MMT, for a sharp and strong peak was found on the curve.

For the samples P0.25-Ti0.1, P0.25-Ti0.2 and P0.25-Ti0.3, the clay added had the same amount of PVP, which was validated by TGA tests; but the clay dispersion states of the samples varied a lot. So the influence of the clay dispersion states on the crystallization behavior of PET/MMT composites could be clarified through the study of these samples. While in the case of the samples P0.25-Ti0.3, P0.5-Ti0.3, and P1.0-Ti0.2, the effects of the amount of the organic clay modifier (PVP) on the crystallization of the nanocomposites could be studied since all these samples possessed almost the same clay dispersion state and the clay added varied in the content of PVP.

Isothermal crystallization

There are many factors that could affect the crystallization of PET, within them, the molecular weight/intrinsic viscosity of the PET matrix is an important one. The intrinsic viscosity of the composites prepared in this study were measured, the results were shown in Table II. It was found that the intrinsic viscosity of the hybrids were close to each other and a little higher than that of pure PET. This result could eliminate the possibility that the difference of molecular weight/intrinsic viscosity of the samples could cause any effect on the crystallization behavior of PET matrix.

The crystallization process of crystalline polymer from melts is usually accompanied by significant heat release that can be measured by DSC.[23] To analyze the DSC results, the relative degree of crystallinity at time *t*, *X(t)*, is defined as follows:

$$X(t) = \frac{X_c(t)}{X_c(t_\infty)} = \frac{\int_0^t \frac{dH(t)}{dt} dt}{\int_0^{t_\infty} \frac{dH(t)}{dt} dt} = \frac{\Delta H_t}{\Delta H_\infty} \quad (1)$$

where dH/dt is the rate of heat evolution; ΔH_t is the heat generated at time t; ΔH_∞ is the total heat generated up to the end of the crystallization process. The curves of relative crystallinity ($X(t)$) of the samples versus crystallization time (t) at 212°C was put together in Figure 3 for comparison. It was obvious that the composites had higher crystallization rates compared with that of pure PET at the same temperature. The same phenomena could be found at other crystallization temperatures. It has been reported that, in polymer matrix, clay platelets could act as both an effective nucleating agent[3,11,24–27] and an impediment of the crystallization process[28–31]; the former could accelerate the crystallization of the polymer matrix while the latter would slow down the crystallization process. As the crystallization rate of PET was increased by the organo-clay, the clay layers must have acted as a heterogeneous nucleation agent for PET.

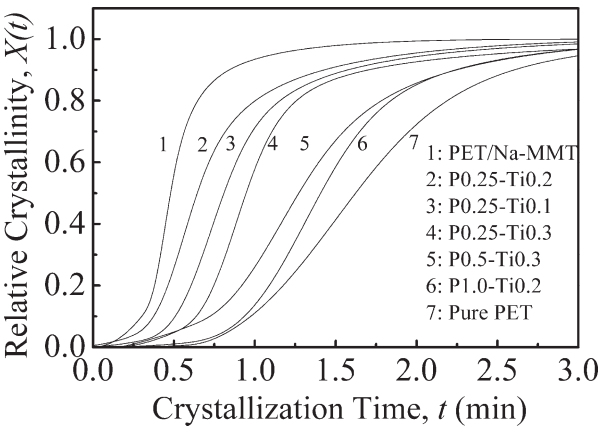

Figure 3 Curves of relative crystallinity ($X(t)$) of the samples versus crystallization time (t) at the crystallization temperature (T_c) of 212°C.

For analysis of the isothermal crystallization, the so-called Avrami equation has been applied.[32,33] Accordingly, the relative crystallinity is related to the crystallization time according to:

$$X(t) = \int_0^t (dH_c/dt)dt \Big/ \int_0^\infty (dH_c/dt)dt = 1 - \exp(-Kt^n) \quad (2)$$

where $X(t)$ is the relative crystallinity at time t, dH/dt is the rate of crystallization heat evolution. The parameter K in eq (2) is an overall crystallization rate constant and n is the Avrami exponent, which is a function of the nucleation process and crystal growth geometry.

The values of n and K could be calculated from fitting to experimental data with the double logarithmic form of eq (2):

$$\log\{-\ln[1 - X(t)]\} = \log K + n \log t \quad (3)$$

The crystallization rate constant K and Avrami exponent n could be determined from the intercept and slope in the plot of $\log\{[-\ln[1 - X(t)]\}$ versus $\log t$. Half time of the crystallization ($t_{1/2}$), another important parameter that could represent the crystallization rates of the composites, could be obtained using the following equation:

$$t_{1/2} = \left(\frac{\ln 2}{K}\right)^{1/n} \quad (4)$$

where K is the overall crystallization rate constant and n is the Avrami exponent.

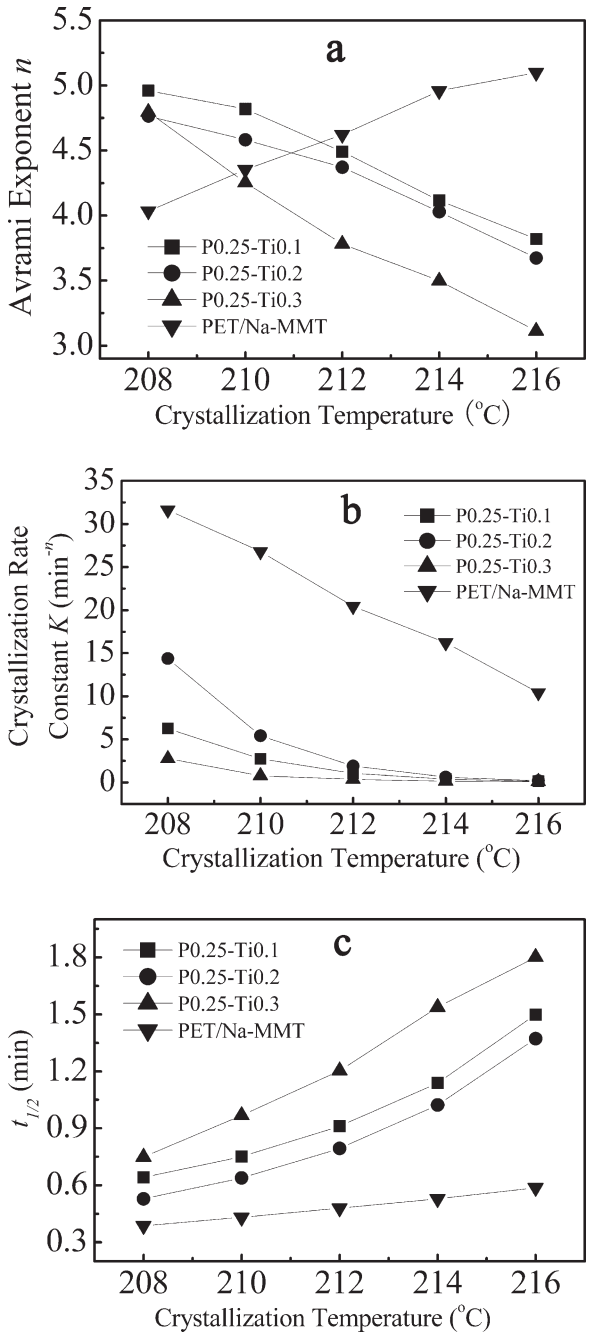

Figure 4 Avrami exponent (n), crystallization rate constant (K) and half crystallization time ($t_{1/2}$) of PET/Na-MMT, P0.25-Ti0.1, P0.25-Ti0.2, and P0.25-Ti0.3 at different crystallization temperatures.

The values of Avrami exponent n, crystallization rate constant K and half crystallization time ($t_{1/2}$) at different crystallization temperatures of the samples PET/Na-MMT, P0.25-Ti0.1, P0.25-Ti0.2 and P0.25-Ti0.3 were shown in Figure 4(a–c), respectively; while the crystallization parameters of the samples pure PET, P0.25-Ti0.3, P0.5-Ti0.3, P1.0-Ti0.2, and 2P0.25-Ti0.3 were illustrated in Figure 5(a–c).

Apparently, as the crystallization temperature increased, the values of K decreased and crystalliza-

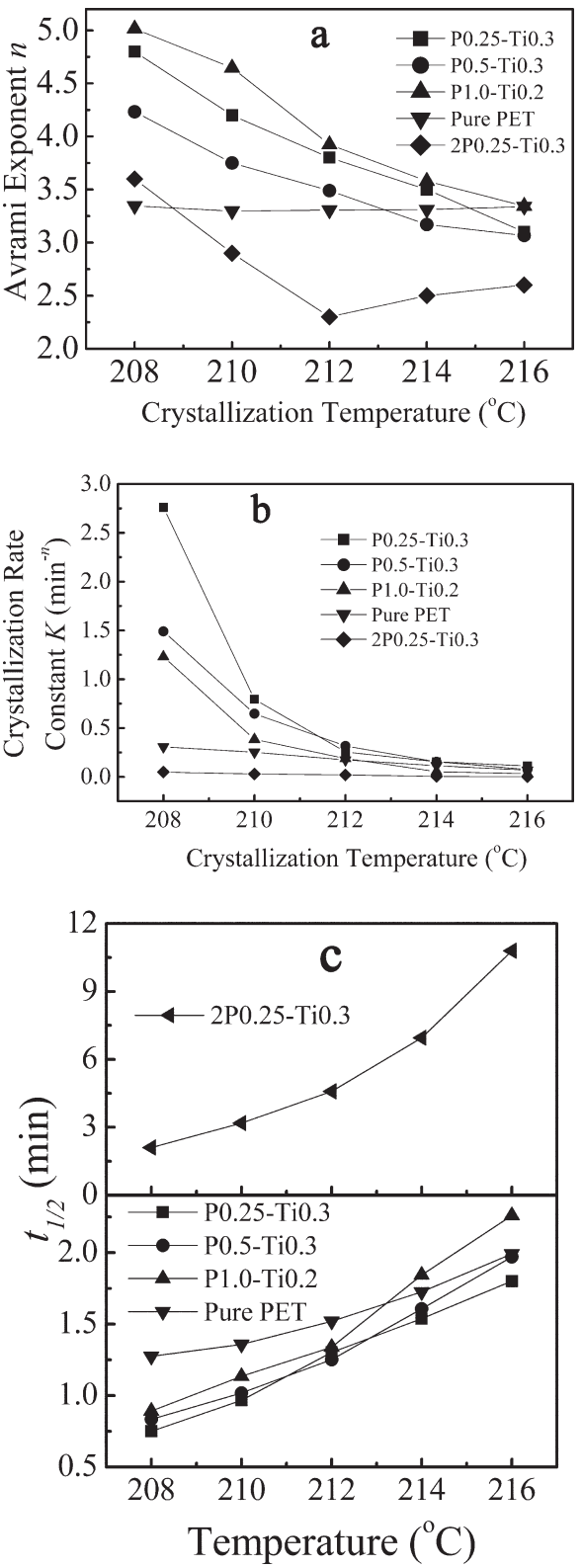

Figure 5 Avrami exponent (n), crystallization rate constant (K) and half crystallization time ($t_{1/2}$) of 2P0.25-Ti0.3, P0.25-Ti0.3, P0.5-Ti0.3, P1.0-Ti0.2, and Pure PET at different crystallization temperatures.

tion half time ($t_{1/2}$) increased for all samples, for the elevated temperature could disturb the diffusion of the polymer chains toward the growth fronts of the spherulites.

The addition of clay remarkably accelerated the crystallization of PET. The values of K for the composites were larger than that of pure PET and $t_{1/2}$ were shorter for the hybrids. However, the crystallization behavior of the PET/MMT composites varied a lot between one another. As the clay loading for all the samples were the same (2 wt %), the treatment of original MMT together with its dispersion states must have great effects on the crystallization behavior of the PET matrix.

First, the clay dispersion state was taken into consideration while the content of clay modifier held constant. According to Figure 4(b,c), exfoliated PET/MMT nanocomposites (P0.25-Ti0.3) had longer $t_{1/2}$ than the agglomerate one (P0.25-Ti0.1) while the intercalated PET/MMT composites (P0.25-Ti0.2) had the shortest $t_{1/2}$. The rate constant K of the intercalated sample ranged from 15 to 0.2 at different crystallization temperatures, much larger than that of the agglomerate and exfoliated samples, so the values of K displayed the same trend as that of $t_{1/2}$. Clearly, intercalated and agglomerate samples crystallized faster than exfoliated ones. This was contradictory to the conclusions of other researchers. Usually, the introduction of MMT would significantly accelerate the crystallization process of the PET substrate due to the heterogeneous nucleation effect. The MMT platelets could act as nucleating agent, initiate the crystallization of the PET matrix. Though, simultaneously, the MMT layers could be some kind of obstacle that impedes the crystal growth, the nucleation effect would be primary in most cases, so the overall crystallization rate that was observed through DSC tests would be faster for the PET/MMT composites. Further, more homogeneous dispersion state of the MMT platelets could magnify the nucleation effect MMT, for in exfoliated PET/MMT nanocomposites, the number of clay layers that actually promoted the crystallization of PET is much bigger than that of intercalated or agglomerated ones and the active surface area of the clay was enlarged by the delamination of clay,[11] resulting in a much more increased crystallization rate, especially when clay content is low.[3,11,15,34–37]

However, in the work of this article, some opposite results were obtained. The incorporation of MMT did increase the crystallization rate of PET, but better clay dispersion state resulted in even lower crystallization rate than that of intercalated and agglomerated PET/MMT composites when clay loading was only 2 wt %, though still higher than that of pure PET. One possible explanation may be suitable for this phenomenon. Above all, it is reasonable to assume that since the clays added into the three samples had the same PVP content, which had been confirmed by TGA results, the nucleation efficiency of the clays should not vary a lot (this assumption was confirmed by nonisothermal DSC and POM tests, which will be shown later), the difference of the overall crystallization rate of the samples should be caused by the difference of the rate of crystal growth. In the agglomerated PET/MMT composites, clay dispersed coarsely throughout the PET substrate, so there were quite a lot of blank spaces in which the clay particles were absent. The growing crystals could hardly encounter MMT layers that might terminate the crystal growth. So the clay particles acted mainly as nucleating agent. As the clay dispersed more homogeneously, that is to say, clay formed an intercalated structure throughout the PET substrate, the number of clay stacks within the PET matrix actually increased; the nucleation effect of the MMT platelets might be improved to some extent. However, there were still big blank areas in which there were hardly any clay layers, so the possibility of the disturbance of the growth of the PET crystal lamellas by MMT sheets was still low. As a result, the overall crystallization process was somewhat faster for the intercalated sample than the agglomerated one. As for the exfoliated samples, there were homogeneously dispersed MMT lamellas all over the nanocomposite, which could produce an obstacle on the polymer chain movement, reduce the tendency for the molecular to be crystallized. Because the MMT layers in P0.25-Ti0.3 had almost the same nucleating efficiency as that of the other two, the crystallization rate of the exfoliated sample was the slowest of the three, for the physical hindrance of MMT layers to PET molecular chains was prominent. To further confirm our expectation, PET/MMT nanocomposites with 4 wt % organo-clay was also prepared (2P0.25-Ti0.3). The clay treatment procedure was the same as P0.25-Ti0.3. XRD curves proved that clay in 2P0.25-Ti0.3 possessed an exfoliated structure. Clearly, it crystallized much more slowly than P0.25-Ti0.3, even slower than pure PET [Fig. 5(b,c)]. This phenomenon validated our assumption. Obviously, 2P0.25-Ti0.3 had a higher density of clay sheets than P0.25-Ti0.3 within the PET substrate, which could force the growing PET crystal lamellas along a more tortuous path or possibly even stop some of them from growing[30]; or, higher amount of silicate layers in 2P0.25-Ti0.3 could hinder the polymer chain motion more severely.[28,29] So, according to the above discussion, delamination of MMT layers could slow down the overall crystallization rate of the PET matrix.

The values of Avrami exponent n seemed not to agree well with Avrami's crystallization theory. According to Avrami, n should equal to 4 for

spherulite in the case of homogeneous nucleation, while $n = 3$ for heterogeneous nucleation. However, the values of n could be larger than 3 for the PET/MMT composites synthesized in this study, which would surely crystallize through heterogeneous nucleation. Bian et al.[38,39] summed up the crystallization modes of PET and proposed that n values relate with the number of growth points in crystal nuclei; namely, the bigger the number is, the larger the n values. The MMT lamellas not only acted as nucleation agent, but also improved the ordering of PET segments from the physical interaction between PET and MMT, resulting in the addition of the crystal growth points, thus increasing the value of Avrami exponent n. Though the dimension of the crystal growth might be less than 3 due to the restriction of the nano-scale dispersed MMT layers in PET/MMT nanocomposites, the Avrami exponent n could be larger than 3 just because the addition of the crystalline growth points due to the MMT layers.

Second, the organification of MMT could also affect the crystallization rate of PET/MMT composites when the MMT possessed the same dispersion state. According to Nam et al.,[40] the organic modifier of MMT would weaken the nucleation effect of MMT platelets due to the shielding effect and/or miscibility between surfactants of clays and polyester chains. For the exfoliated samples P0.25-Ti0.3, P0.5-Ti0.3, and P1.0-Ti0.2, the clay dispersion states were almost the same based on XRD tests, so the retarding effect on the crystallization process exerted by clay platelets should be almost the same. However, the crystallization rate went slower as the PVP content of the treated MMT increased. As shown by Figure 5(b,c), at the same isothermal crystallization temperature, the crystallization rate constant K went smaller as the clay added into the nanocomposites containing more PVP; also, $t_{1/2}$ went longer. Besides, according to Figure 4, for PET/Na-MMT and P0.25-Ti0.1, clay formed big grains in PET substrate for both samples, but the crystallization rate was much faster for the hybrids based on the unmodified MMT. So, it was evident that PVP could weaken the potential of MMT layers as nucleating agent for PET; clay treated with more PVP was less effective in accelerating the crystallization of PET. To sum up, the incorporation of PVP could impair the nucleating efficiency of the clay, more PVP would result in an even lower nucleation activity. Similarly, it was observed that the Avrami exponent n for the composites might be larger than 3 according to Figure 5(a).

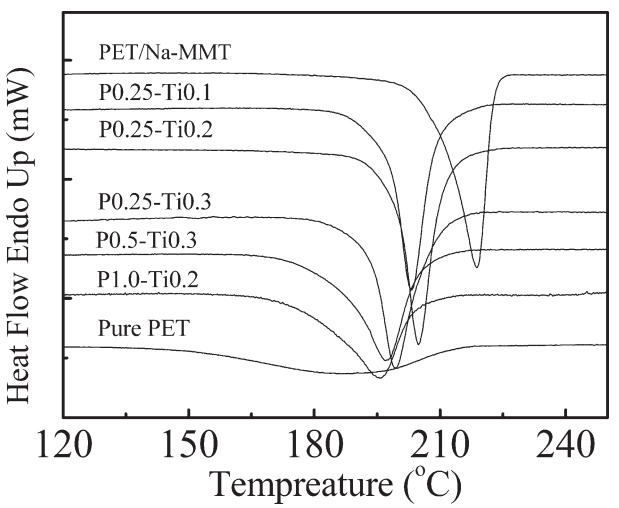

Figure 6 Cooling DSC curves of Pure PET and PET/MMT composites at 10°C/min.

TABLE V
Nonisothermal DSC Results of Pure PET and PET/MMT Composites

Samples	T_c (°C)	T_{on} (°C)	$t_{1/2}$ (min)	ΔH_c (J/g)
PET/Na-MMT	218.7	222.8	0.64	49.2
P0.25-Ti0.1	203.2	209.2	0.74	45.0
P0.25-Ti0.2	204.8	211.5	0.76	48.1
P0.25-Ti0.3	199.3	210.6	1.23	43.9
P0.5-Ti0.3	197.6	205.1	1.33	41.8
P1.0-Ti0.2	196.5	204.5	1.58	36.6
Pure PET	193.3	201.7	1.69	38.9

Nonisothermal crystallization

In the above discussion, there was an important hypothesis that MMT treated with the same amount of PVP should have approximately the same heterogeneous nucleation efficiency. The onset temperature (T_{on}), which is the temperature where the thermograph departs from the base line during a nonisothermal cooling scan, has been used to quantitatively describe the ability of the organo-clays to initiate the crystallization of the polymer matrix in a polymer/clay hybrid system.[30,40,41] Higher T_{on} usually means a stronger nucleation effect. Figure 6 showed the cooling curves of various PET/MMT composites and pure PET at 10°C/min from the melt to 50°C after been held at 290°C for 5 min to eliminate any thermal history. The values of T_{on}, T_c (the temperature where the exotherm shows the peak) and $t_{1/2}$ (half crystallization time) were listed in Table V. Half crystallization time $t_{1/2}$ can be obtained using the following formula:

$$t_{1/2} = (T_{on} - T_{1/2})/x \quad (5)$$

where χ is the cooling rate (°C/min), $T_{1/2}$ is the temperature (°C) at which the relative degree of crystallization $X(t)$ is 50%.

According to Table V, it was evident that all the samples which contained MMT have higher T_{on}

than pure PET during the cooling DSC scan. So, MMT, no matter treated or not, could successfully act as the nucleation agent for PET. However, PET hybrids containing pristine MMT had the highest T_{on}, 21 and 12 degrees higher than that of pure PET and the exfoliated sample P0.25-Ti0.3 respectively, which meant that pure MMT had the strongest ability to initiate the crystallization of PET. Once the clay was treated with PVP, the heterogeneous nucleation ability of the clay layers was greatly weakened; more PVP would result in lower nucleation efficiency. As indicated by Table V, the hybrids containing organo-clay with less PVP had higher T_{on} in the programmed cooling process, for example, T_{on} of P0.25-Ti0.3 was 6 degrees higher than that of P1.0-Ti0.2. For the clays treated with the same amount of PVP (P0.25-Ti0.1, P0.25-Ti0.2, and P0.25-Ti0.3), the T_{on} of the corresponding composites were almost the same, which validated the assumption mentioned above. Though the amount of TiO_2/SiO_2 sol introduced into the organo-clay varied from one another and TiO_2 and SiO_2 particles did have some nucleation effect for PET,[42,43] the samples containing more TiO_2/SiO_2 sol, such as P0.25-Ti0.3, seemed not to have a faster initial crystallization rate. This might be caused by the fact that the amount of TiO_2/SiO_2 sol was too small relative to MMT that added into the PET/MMT hybrids, the difference of the quantity of the TiO_2/SiO_2 sol was far from enough to affect the macroscopic crystallization process. Furthermore, it was clear that the in the range of this study, clay dispersion state had little effect on the heterogeneous nucleation ability of MMT, the amount of PVP that introduced on the MMT platelets was the primary factor which could determine the rate of the heterogeneous nucleation process. This might be caused by the shielding effect exerted by the organic clay modifier.[27,40,44,45] Though more clay layers should result in more PET nucleus in exfoliated samples, the smaller size of the MMT platelets might make it harder to trigger the crystallization of PET.[46]

In the programmed cooling DSC scan, T_c and half crystallization time ($t_{1/2}$) were the indicators of the overall crystallization rate attributed to the combine of nucleation and crystal growth. The results of the nonisothermal DSC tests matched well with the isothermal DSC studies according to Table V. PET added with pristine MMT had the highest T_c and shortest $t_{1/2}$, indicating highest crystallization rate. As the clay filler been pretreated with more and more PVP, T_c became lower and $t_{1/2}$ grew longer. In the case of the samples in which MMT was treated with the same amount of PVP but MMT possessed different clay disperse state, more homogenous clay dispersion would bring on slower crystallization rate.

TABLE VI
The Time at which the First Crystal Nucleus Presented During the Cooling Process of the POM Study

Samples	Time (s)[a]
PET/Na-MMT	300
P0.25-Ti0.1	308
P0.25-Ti0.2	312
P0.25-Ti0.3	308
P0.5-Ti0.3	320
P1.0-Ti0.2	324
Pure PET	332

[a] The time counting started once the cooling process began.

The heat of crystallization (ΔH_c) of the samples released during this nonisothermal process was determined from the area of crystallization peak under the DSC curves. The values of ΔH_c of the samples were recorded in Table V. For the hybrids, it was found that the samples with faster isothermal/nonisothermal crystallization rates had larger ΔH_c values. For the samples PET/Na-MMT, P0.25-Ti0.1, and P0.25-Ti0.2, the clay added displayed prominent heterogeneous nucleation effects, and the impediments of the crystallization process caused by MMT platelets was negligible, so these samples had higher crystallinity and ΔH_c. As the clay lamellas dispersed more homogeneously within the PET substrate, clay layers might make the polymer chain more difficult to be crystallized, so the ΔH_c went lower for P0.25-Ti0.3, P0.5-Ti0.3, and P1.0-Ti0.2. For the sample P1.0-Ti0.2, the value of ΔH_c was even lower than that of pure PET.

Crystalline morphology

Polarizing optical micrograph (POM) is by far the simplest way to directly observe the crystallization process of polymers. When PET or PET/MMT composites are in the melt state, only dark background could be seen with a polarized optical microscope. As soon as the PET substrate started crystallization, the typical "Maltase Cross" should be observed. However, PET spherulites were too small for the clear spherulites morphologies to be seen. So, once there was PET spherulites appeared within the view of the microscope, only some bright crystal nuclei could be observed. As a result, when the samples prepared in this study were being programmed cooled from the melt state with a polarized microscope to perform on-line observation, the time at which the first crystal nucleus presented could be considered as an indicator of how strong the heterogeneous nucleation existed in the samples. By carefully comparing the POM images of pure PET and the composites captured during the cooling scan (10°C/min) from the melt state, the times at which

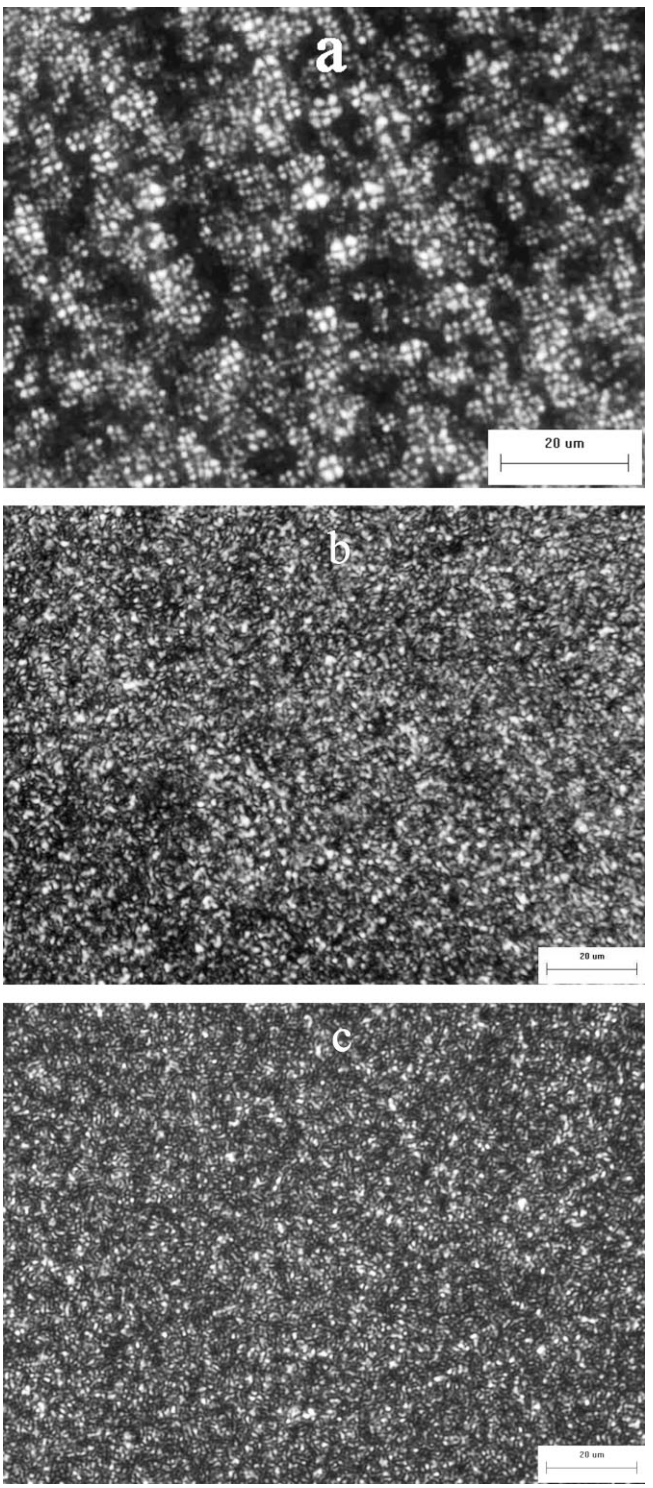

Figure 7 Crystal morphology of the samples: (a) Pure PET, (b) PET/Na-MMT, and (c) P0.25-Ti0.3.

the initial small nucleus could be seen were pointed out and recorded in Table VI. Obviously, according to Table VI, during the nonisothermal process, the sample PET/Na-MMT needed the shortest time to form the initial small spherulites which meant that pure MMT had the strongest heterogeneous nucleation effect. In the case of the composites in which the clay had been treated, it took longer time for the first spherulites to appear. As expected, pure PET took the longest time to form the crystal nucleus. These results matched well with the nonisothermal DSC data. Further, the crystal morphologies of pure PET, PET/Na-MMT, and P0.25-Ti0.3 were studied. Figure 7 showed the images taken after the samples were held at 230°C for 60 min under the protection of dry nitrogen. Clearly, for pure PET, typical Maltese Cross patterns could be easily discerned, the spherulites sizes were fairly big and uniform. The addition of pristine MMT apparently decreased the size of PET crystals [Fig. 7(b)]. Moreover, for the exfoliated sample P0.25-Ti0.3 [Fig. 7(c)], the crystallites were even smaller, irregularly shaped, interlocked with each other, and no clear boundaries between two crystallites could be observed. This result, to some extent, further confirmed that clay

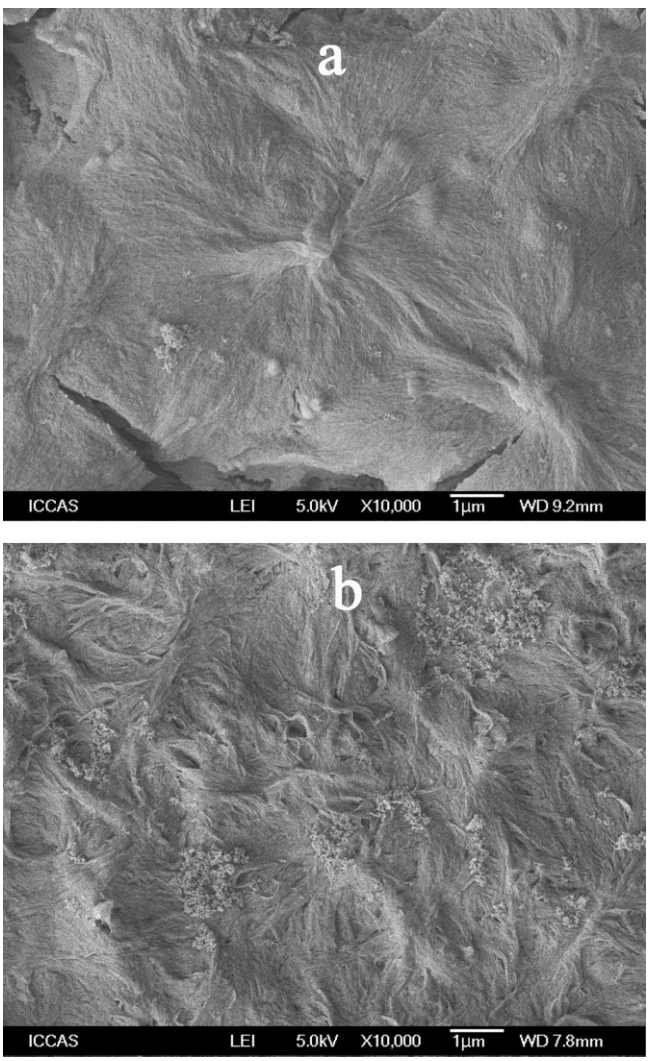

Figure 8 SEM photographs of etched surface for (a) neat PET, (b) P0.25-Ti0.3 after isothermal crystallizing at 230°C for 60 minutes.

particles could reduce the mobility of polymer chains, cause a retarding effect on the crystal growth of PET matrix.

The morphologies of crystallized neat PET and PET/MMT nanocomposite were also studied by SEM. Figure 8 exhibited the SEM photographs of etched surfaces of neat PET and P0.25-Ti0.3 after isothermal crystallization at 230°C for 60 min. Apparently, for pure PET, the well defined radical texture of PET spherulites could be easily discerned, the boundaries between the neighboring were clear, as shown by Figure 8(a). However, in the case of P0.25-Ti0.3 [Fig. 8(b)], most of the crystallites were relatively small, irregularly shaped, the crystal lamellas were distorted and interlocked with each other; also the boundaries were obscure. So, the crystal growth was mainly terminated by clay layers rather than crystal impingement.[12] As a result, MMT layers could act as noncrystallisable barriers which could disturb crystal growth by forcing the growing lamellar stacks along a more tortuous growth path or even stop several from growing. The growth and perfection of PET crystals could be impeded by the silicate layers.

CONCLUSIONS

A series of PET/MMT composites were prepared using these MMT treated by TiO_2/SiO_2 sol and PVP as polycondensation catalysts. XRD results revealed that MMT dispersion state in PET matrix varied a lot according to different clay treatments.

DSC, POM, and SEM studies clearly indicated that MMT could act as both heterogeneous nucleating agents and hindrance of the growing PET crystals no matter how the clay was treated. However, the amount of PVP absorbed on MMT could affect the strength of the nucleation effects of MMT and clay dispersion states could influence the intensity of the confinements on the polymer chain movements. Thus, clay treatment determined which effect of MMT would be primary on the crystallization process of PET: acceleration or impediment.

When clay agglomerated in PET substrate, the physical hindrance of MMT layers was negligible, so the composites had very high crystallization rates. As the nucleation strength could be weakened by the absorbed PVP, it was clear that PET/Na-MMT crystallized faster than P0.25-Ti0.1.

If the MMT platelets were thoroughly delaminated into the PET matrix, the intensity of spatial constraint exerted by MMT was very strong, the growing spherulites were possibly to be terminated by clay sheets. So, for the exfoliated PET/MMT nanocomposites, MMT mainly acted as hindrance of PET crystallization, the overall crystallization rate was slow. For 2P0.25-Ti0.3, the density of the clay layers was the highest among all the PET/MMT composites synthesized in this study, the crystallization rate of this sample was even slower than pure PET.

Based on the above discussion, influences of the crystallization rate of PET/MMT composites were clarified. Also, the results provided a possible way to solve the problem that PET/MMT composites crystallized too fast in some conditions, giving this study some practical meanings.

References

1. Chang, J. H.; Kim, S. J.; Joo, Y. L.; Im, S. Polymer 2004, 45, 919.
2. Li, Y.; Ma, J. H.; Wang, Y. M.; Liang, B. R. J Appl Polym Sci 2005, 98, 1150.
3. Ke, Y. C.; Long, C. F.; Qi, Z. N. J Appl Polym Sci 1999, 71, 1139.
4. Ou, C. F.; Ho, M. T.; Lin, J. R. J Polym Res 2003, 10, 127.
5. Imai, Y.; Nishimura, S.; Abe, E.; Tateyama, H.; Abiko, A.; Yamaguchi, A.; Aoyama, T.; Taguchi, H. Chem Mater 2002, 14, 477.
6. Tsai, T. Y.; Li, C. H.; Chang, C. H.; Cheng, W. H.; Hwang, C. L.; Wu, R. J. Adv Mater 2005, 17, 1769.
7. Choi, W. J.; Kim, H. J.; Yoon, K. H.; Kwon, O. H.; Hwang, C. I. J Appl Polym Sci 2006, 100, 4875.
8. Kim, S. H.; Kim, S. C. J Appl Polym Sci 2007, 103, 1262.
9. Hao, J. Y.; Lu, X. H.; Liu, S. L.; Lau, S. K.; Chua, Y. C. J Appl Polym Sci 2005, 101, 1057.
10. Chang, J. H.; Mun, M. K. Polym Int 2007, 56, 57.
11. Saujanya, C.; Imai, Y.; Tateyama, H. Polym Bull 2003, 51, 85.
12. Wan, T.; Chen, L.; Chua, Y. C.; Lu, X. H. J Appl Polym Sci 2004, 94, 1381.
13. Calcagno, C. I. W.; Mariani, C. M.; Teixeira, S. R.; Mauler, R. S. Polymer 2007, 48, 966.
14. Wang, Y. M.; Shen, C. Y.; Li, H. M.; Li, Q.; Chen, J. B. J Appl Polym Sci 2004, 91, 308.
15. Saujanya, C.; Imai, Y.; Tateyama, H. Polym Bull 2002, 49, 69.
16. Wu, T. B.; Ke, Y. C. Thin Solid Films 2007, 515, 5220.
17. Phang, I. Y.; Pramoda, K. P.; Liu, T. X.; He, C. B. Polym Int 2004, 53, 1282.
18. Yamanaka, S.; Inoue, Y.; Hattori, M.; Okumura, F.; Yoshikawa, M. Bull Chem Soc Jpn 1992, 65, 2494.
19. Han, Y. S.; Matsumoto, H.; Yamanaka, S. Chem Mater 1997, 9, 2013.
20. Guan, G. H.; Li, C. C.; Zhang, D. J Appl Polym Sci 2005, 95, 1443.
21. Tsipursky, S.; Beall, G. W.; Sorokin, A.; Goldman, A.U.S. Pat. 5,721,306, 1998.
22. Han, Y. S.; Yamanaka, S.; Choy, J. H. J Solid State Chem 1999, 144, 45.
23. Achilias, D. S.; Papageorgiou, G. Z.; Karayannidis, G. P. J Polym Sci, Part B: Polym Phys 2004, 42, 3775.
24. Ogata, N.; Jimenez, G.; Kawai, H.; Ogihara, T. J Polym Sci Part B: Polym Phys 1997, 35, 389.
25. Maiti, P.; Nam, P. H.; Okamoto, M.; Hasegawa, N.; Usuki, A. Macromolecules 2002, 35, 2042.
26. Nam, J. Y.; Ray, S. S.; Okamoto, M. Macromolecules 2003, 36, 7126.
27. Krikorian, V.; Pochan, D. J. Macromolecules 2004, 37, 6480.
28. Lincoln, D. M.; Vaia, R. A.; Wang, Z. G.; Hsiao, B. S. Polymer 2001, 42, 1621.
29. Fornes, T. D.; Paul, D. R. Polymer 2003, 44, 3945.
30. Homminga, D.; Goderis, B.; Dolbnya, I.; Reynaers, H.; Groeninckx, G. Polymer 2005, 46, 11359.

31. Wu, D. F.; Zhou, C. X.; Fan, X.; Mao, D. L.; Bian, Z. J. Appl Polym Sci 2006, 99, 3257.
32. Avrami, M. J. Chem Phys 1939, 7, 1103.
33. Avrami, M. J. Chem Phys 1941, 9, 177.
34. Xu, J. T.; Zhao, Y. Q.; Wang, Q.; Fan, Z. Q. Polymer 2005, 46, 11978.
35. Xu, J. T.; Wang, Q.; Fan, Z. Q. Eur Polym J 2005, 41, 3011.
36. Liu, X. H.; Wu, Q. J. Eur Polym J 2002, 38, 1383.
37. Hu, X. B.; Lesser, A. J. J Polym Sci Part B: Polym Phys 2003, 41, 2275.
38. Bian, J.; Ye, S. R.; Feng, L. X. Chem J Chin Univ 2000, 21, 1481.
39. Bian, J.; Ye, S. R.; Feng, L. X. J Polym Sci Part B: Polym Phys 2003, 41, 2135.
40. Nam, P. H.; Ninimiya, N.; Fujimori, A.; Masuko, T. Polym Eng Sci 2006, 46, 39.
41. Homminga, D.; Goderis, B.; Dolbnya, I.; Reynaers, H.; Groeninckx, G. Polymer 2006, 47, 1620.
42. Groeninckx, G.; Berghmans, H.; Overbergh, N. J Polym Sci Polym Phys Ed 1974, 12, 303.
43. Lu, H.; Wang, H. L.; Zheng, A. N.; Xiao, H. N. Polym Composite 2007, 28, 42.
44. Tanaka, G.; Goettler, L. A. Polymer 2002, 43, 541.
45. Fornes, T. D.; Hunter, D. L.; Paul, D. R. Macromolecules 2004, 37, 1793.
46. Xiao, J. F.; Hu, Y.; Wang, Z. Z.; Tang, Y.; Chen, Z. Y.; Fan, W. C. Eur Polym J 2005, 41, 1030.